RF Dipole Coil with Novel Slotted Shielding Plate Achieving an Improved B1 Distribution for 7 T MRI

Zhichao Chen[1,2], Mahdi Abbasi[1], Klaus Solbach[2], Daniel Erni[1], and Andreas Rennings[1]

[1]*General and Theoretical Electrical Engineering (ATE), Faculty of Engineering, University of Duisburg-Essen, Duisburg, NRW, Germany,* [2]*High Frequency Engineering (HFT), Faculty of Engineering, University of Duisburg-Essen, Duisburg, NRW, Germany*

TARGET AUDIENCE: Researchers interested in RF coil designs for ultra-high-field magnetic resonance imaging.

PURPOSE: Recently, multi-channel RF coils based on several longitudinally oriented strip-line elements have been successfully applied in ultra-high field magnetic resonance imaging (MRI) [1, 2, 3]. In comparison to the 25 cm-long element in [2], where the meanders were connected to an adjacent metal plate (2 cm away from the coil) by using a so-called end-capacitor, a novel 41 cm-long design with an eigen-resonant shielding plate has been presented in [4]. Instead of the direct lumped-element-connection between meanders and the shielding plate a field-based coupling is used, which enables the shielding plate to resonate in its natural half-wavelength eigen-mode. Additionally, a dielectric loading of the meander section has been utilized to fine-tune the current distribution on the dipole by increasing its electrical length. A 4-channel RF coil based on this novel element exhibits an improved transversal B_1 homogeneity and an extended longitudinal field-of-view (FoV) [5]. However, for certain local imaging applications the coil elements should be kept compact (smaller than 41 cm) under the consideration of the placement flexibility. Without diminishing the merit of the eigen-resonance of the shielding plate, here in this paper we present an approach to miniaturize the eigen-resonant shielding plate.

METHODS: Fig. 1 shows the proposed dipole coil element. The stripline dipole and the corresponding shielding plate are printed on 0.5 mm-thick Rogers RO4003 substrates (ε_r = 3.55), which are separated by 2 cm of air. The geometry of the strip-line remains unchanged in comparison to the coil element in [2], except that the end-capacitors and the metallic connections are removed. The layout of the miniaturized shielding plate with the geometry data is given in Fig. 1(b). The size reduction of the eigen-resonant shielding plate is achieved by etching several slots in the shielding plate and enclosing the slotted section with high-dielectric substrates (ε_r = 10.9). In order to determine the corresponding eigen-resonant frequency, the shielding plate is illuminated by an incident plane wave, and the current flowing through the transverse cross section of the plate is calculated based on integration of surrounding magnetic field. The eigen-resonant frequency of the shielding plate can be indicated by the local maximum of the integrated current. The slotted and ordinary (unslotted) shielding plates are compared based on single coil element and a 4-channel coil array. For the single-element based comparison, a flat phantom (ε_r = 58.2, σ = 0.92 S/m) is placed 2 cm above the coil element to mimic the human body at 300 MHz. The transversal magnetic field distribution inside the phantom is normalized to the square root of peak SAR and plotted in dB. Subsequently, a 4-channel coil array consisting of the proposed dipole elements with slotted shielding plates is presented and compared with the ordinary (unslotted) case based on FDTD simulations. The corresponding coil array is loaded by a homogenous cylindrical phantom with a diameter of 20 cm. The separation distance from surface of the phantom to the coil element is set to 2 cm. In order to excite the first CP mode, the coil elements in our case are fed equally in magnitude and with a relative phase lag of 90°. For the experimental validation, the magnetic field distribution along a transversal path for different penetration depth (d = 1 cm, 3 cm, 5 cm) inside the liquid-based phantom is measured and normalized to the square root of peak SAR.

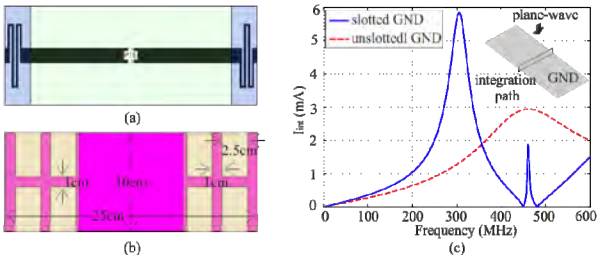

Fig. 1: Layouts of the (a) stripline dipole and (b) the slotted shielding plate. (c) The integrated current on the slotted and unslotted shielding plate under an excitation of a normal incident plane wave.

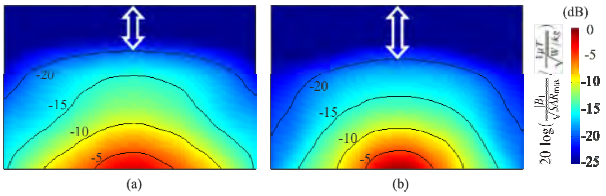

Fig. 2: Simulated transverse $|B_1|$ distribution of a dipole coil with (a) slotted and (b) unslotted shielding plate. The field distribution is normalized to the square root of peak SAR and plotted in dB.

RESULTS AND DISCUSSION: As shown in Fig. 1(c), the ordinary (unslotted) shielding plate exhibits a half-wavelength eigen-resonance at 465 MHz. The slots in the shielding plate create high inductance which brings down the eigen-resonant frequency. Additionally, the high-dielectric substrate (with an optimal thickness of 1.5 cm atop and beneath the slotted sections) further increases the electrical length of the path where the eigen-resonant current flows. As a result, the eigen-resonance frequency is brought down to 300 MHz. Due to this eigen-current on the shielding plate, the magnetic field inside the phantom of the coil element with slotted shielding plate is distributed in a broader manner compare to the ordinary element (cf. Fig. 2). Additionally to the broader field distribution, the penetration depth of magnetic field is slightly increased as well. For the 4-channel coil, the transversal B_1^+ homogeneity of the RF coil based on the element with slotted shielding plate is improved in comparison to the case of ordinary shielding plate (cf. Fig. 3). Specifically, the coefficient of variation of the absolute transversal B_1^+ in the case of slotted and ordinary shielding plate reads 0.38 and 0.43, respectively. According to the measured B_1 field distribution along a transverse path (cf. Fig. 4), the proposed slotted shielding plate (with 3 mm and 6 mm Arlon AD1000 substrate atop and beneath the slotted sections, respectively) provides a broader field distribution and an increased penetration comparing to the ordinary case, which show a good agreement on the simulations. It can be noticed that the improvement due to the slotted eigen-resonant shielding plate degrades with an increased penetration depth.

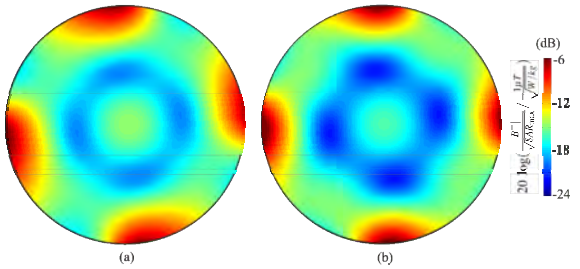

Fig. 3: Simulated transverse $|B_1^+|$ distribution of a 4-channel dipole coil with (a) slotted and (b) unslotted shielding plate. The field distribution is normalized to the square root of peak SAR and plotted in dB.

CONCLUSION: Here we presented a dipole coil with miniaturized eigen-resonant shielding plate by etching several slots in the shielding plate and enclosing the slotted section with high-dielectric substrates. The proposed dipole coil exhibits an improvement in terms of B_1 homogeneity and penetration depth comparing to the ordinary (unslotted) case, which has been confirmed by the experimental results.

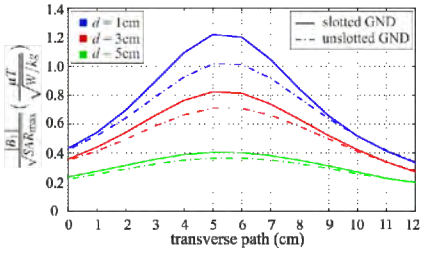

Fig. 4: Measured B_1 distribution along a transverse path for different penetration depth (d =1, 3, 5 cm).

REFERENCES: [1] D. O. Brunner et al., Proc. ISMRM 15 (2007), 448. [2] S. Orzada et al., Proc. ISMRM 16 (2008), 2979. [3] A. J. E. Raaijmakers et al., MRM, vol. 66, pp. 1488-1497, 2011. [4] Z. Chen et al., Int. Microwave Symposium (IMS 2013), WE1E-2, 2013. [5] Z. Chen et al., European Microwave Conference (EuMC 2014), EuMC25-02, 2014.